Tellus (2001), 53A, 27–34

TELLUS
ISSN 0280–6495

A note on using the accelerated convergence method in climate models

By DAILIN WANG, *International Pacific Research Center*, School of Ocean and Earth Science and Technology, University of Hawaii at Manoa, 2525 Correa Road, Honolulu, Hawaii 96822, USA*

(Manuscript received 6 September 1999; in final form 10 July 2000)

ABSTRACT

Application of the accelerated convergence (or asynchronous integration) method of Bryan (1984) to climate problems with time-dependent forcing is investigated using an ocean general circulation model (GCM), with an idealized box ocean and forced with an idealized seasonal restoring surface temperature. Numerical experiments consist of a control experiment, which is integrated synchronously for 9000 years, and 2 experiments with asynchronous integration, one with depth dependent acceleration and one with depth independent acceleration. The latter 2 cases were integrated synchronously for 9000 years after asynchronous equilibria are reached. It is found that a few thousand years of synchronous integration is needed to reach a new equilibrium after asynchronous equilibrium is obtained, consistent with a scaling argument. However, at the new equilibrium, temperature in the deep ocean only differs from that of the early stage of synchronous adjustment by about 0.01°C. So for practical purposes, 50 years of synchronous integration beyond asynchronous equilibrium is sufficient. A simple interpretation of the accelerated convergence method of Bryan is also presented.

1. Introduction

Bryan (1984) developed an accelerated convergence method to speed up the convergence of thermohaline spin-up numerical experiments. The acceleration of convergence is achieved by integrating a distorted physical system, namely, using different time-steps for velocity and for tracers (so-called asynchronous integration). The distorted system has the same form as that of the original physical system if time-derivatives are dropped. For steady forcing, the underlying assumption is that a unique steady state exists. For time-dependent forcing, it is not obvious this technique should work. The need to use time-dependent forcing for climate studies prompted a recent study by Danabasoglu et al. (1996) to address this question. They found that "the model attains synchronous equilibrium in about 15 years provided that a near equilibrium state has been achieved with acceleration". They also found that the annual-mean state of the synchronous equilibrium solution is very close to the mean state of the asynchronous equilibrium solution. These conclusions were reached although synchronous integration was not carried out long enough to demonstrate that a new equilibrium was indeed reached. Based on scaling argument, any adjustment to new equilibrium should take thousands of years, or the diffusive time scales of the system. So a key question is whether the small drift found in Danabasoglu et al. is transient in nature or is representative of long time behavior. For the latter

Corresponding author address: Dr. Dailin Wang, IPRC/SOEST, University of Hawaii at Manoa, 2525 Correa Road, Honolulu, Hawaii 96822.
e-mail: wangd@soest.hawaii.edu

* International Pacific Research Centre is partly sponsored by the Frontier Research System for Global Change.

to be true, the following are implied: (1) the annual mean state is insensitive to the choice of acceleration parameters (or asynchronous time-steps for tracers) and (2) the annual mean state of the asynchronous equilibrium is equal to or very close to the annual mean state of the true equilibrium. Without synchronously integrating the physical system to equilibrium, these two statements cannot be verified. In other words, they are simply assumptions or hypotheses.

In this study, we reinvestigate this problem in a more thorough manner, using a GCM with a simple box-type configuration and simplistic seasonal forcing. To address the question (hypothesis 1) whether or not the mean state of the asynchonous equilibrium is sensitive to the choice of acceleration parameters, we conduct two asynchronous experiments, one has depth dependent time-step for temperature and one does not. After asynchronous integration reached equilibrium, synchronous integration is carried out long enough such that a new equilibrium is reached to test the hypothesis 2. A control experiment is also integrated from rest to equilibrium synchronously. To our knowledge, this is a first such integration using a GCM.

A simple interpretation of the accelerated convergence method of Bryan (1984) is given in Section 2. Numerical experiments and model results are described in Section 3. Some concluding remarks are made in Section 4.

2. An interpretation of the accelerated convergence method of Bryan

The distorted system of Bryan (1984) is formed by introducing two extra parameters, α and γ in the momentum and tracers equations. These two parameters, in general, can be functions of spatial variables. The equations of the distorted system are

$$\boldsymbol{u}_{\mathrm{t}} + \frac{1}{\alpha}\left(\boldsymbol{u}\cdot\nabla\boldsymbol{u} + \boldsymbol{u}w_z + f\boldsymbol{k}\times\boldsymbol{u} + \frac{\nabla p}{\rho_0} - A_{\mathrm{h}}\nabla^2\boldsymbol{u} - A_{\mathrm{v}}\boldsymbol{u}_{zz}\right) = 0, \qquad (1)$$

for momentum and

$$\rho_{\mathrm{t}} + \gamma\left(\boldsymbol{u}\cdot\nabla\rho + w\rho'_z - \frac{\rho_0}{g}N^2 w - K_{\mathrm{h}}\nabla^2\rho - K_{\mathrm{v}}\rho_{zz}\right) = 0, \qquad (2)$$

for potential density, where $\boldsymbol{u}$ is horizontal velocity, w is vertical velocity, p is pressure, A_{h} and A_{v} are horizontal and vertical eddy viscosity coefficients, N is the background Brunt–Väisälä frequency, ρ' is the deviation of density from the background density (e.g., annual mean), K_{h} and K_{v} are horizontal and vertical eddy diffusivity coefficients, ∇ and ∇^2 are horizontal gradient and Laplacian operators. For simplicity, we neglect salinity (or equivalently, assuming density is a linear function of potential temperature and salinity). We cast the heat equation (2) in terms of potential density for the convenience of discussion. The actual model heat equation is cast in potential temperature.

Following Bryan (1984), introducing a stretched time $t' = t/\alpha$, (1) and (2) become

$$\boldsymbol{u}_{\mathrm{t}'} + \boldsymbol{u}\nabla\cdot\boldsymbol{u} + \boldsymbol{u}w_z + f\boldsymbol{k}\times\boldsymbol{u} + \frac{\nabla p}{\rho_0} - A_{\mathrm{h}}\nabla^2\boldsymbol{u} - A_{\mathrm{v}}\boldsymbol{u}_{zz} = 0, \qquad (3)$$

$$\rho_{\mathrm{t}'} + \alpha\gamma(\boldsymbol{u}\cdot\nabla\rho + w\rho'_z - K_{\mathrm{h}}\nabla^2\rho - K_{\mathrm{v}}\rho_{zz}) - \alpha\gamma\frac{\rho_0}{g}N^2 w = 0. \qquad (4)$$

For the case of $\gamma = 1$ and $\alpha > 1$, Bryan (1984), who used temperature equation, showed that the frequency bands of gravity and Rossby waves will be reduced and at the same time local heat capacity of the distorted system is reduced. From (3) and (4), the effects of α and γ can be combined into one parameter $\alpha\gamma$, which we call γ in this study. We next present an equivalent but simpler interpretation of the method developed by Bryan (1984).

For thermohaline spin-up experiments with time-invariant forcing, the time scales to reach steady states for the original physical system and the distorted system are determined by the diffusive time scales

$$\tau_{\mathrm{o}} = H^2/K_{\mathrm{v}}, \qquad \tau_{\mathrm{d}} = H^2/(\gamma K_{\mathrm{v}}), \qquad (5)$$

where H is the depth of the ocean, subscripts $_{\mathrm{o}}$ and $_{\mathrm{d}}$ stand for the original and distorted systems. If horizontal diffusion coefficients are the control parameters, similar time scales can be defined.

For explicit time differencing employed in the GFDL model, the time-steps of integration are determined by the CFL criteria (Courant et al., 1928)

$$\Delta t_{\mathrm{o}} \leqslant \Delta x/C, \qquad \Delta t_{\mathrm{d}} \leqslant \Delta x/(\sqrt{\gamma}C), \qquad (6)$$

for the physical and distorted systems, respectively. Note that when stratification is increased by γ, the phase speed C of linear Kelvin waves (or gravity waves) is increased by $\sqrt{\gamma}$, thus the factor in the second expression of (6). We implicitly assumed that the planetary waves of the systems are linear, as in the analysis of Bryan (1984). As long as C is qualitatively representative of the maximum possible phase speed of the fastest baroclinic planetary waves of the system, the present analysis will be valid.

The number of time-steps of integration needed to reach equilibrium are

$$n_o = \frac{\tau_o}{\Delta t_o} = \frac{H^2 C}{K_v \Delta x}, \qquad n_d = \frac{\tau_d}{\Delta t_d} = \frac{H^2 C}{\sqrt{\gamma} K_v \Delta x}, \tag{7}$$

for the physical and distorted systems, respectively. Eq. (7) is a key point of this section, namely, it is the number of iterations needed to reach equilibrium that determines the efficiency of the accelerated convergence technique (Wang, 1993).

For $\gamma > 1$, the effective eddy diffusivity coefficients (γK_h and γK_v) in (4) are increased, or the diffusive time scales are reduced. The phase speeds of waves are also increased in the distorted system because the stratification is increased by a factor of γ. This means a smaller time-step (for the stretched time t') must be used. However, the number of time-steps needed to reach equilibrium is reduced according to (7). The speed up factor is

$$e = n_o/n_d = \sqrt{\gamma} > 1, \qquad \text{for } \gamma > 1. \tag{8}$$

The time-step is also controlled by the advective velocity. For the distorted system, the following must also be satisfied.

$$\Delta t_d \leqslant \Delta x/(\gamma U), \tag{9}$$

where U is an advective velocity scale of the distorted system. Further acceleration of convergence stops when $\gamma U \geqslant \sqrt{\gamma} C$. So, the optimal acceleration coefficient γ satisfies

$$(\gamma U) = \sqrt{\gamma} C, \tag{10}$$

$$\text{or} \qquad \gamma = \frac{C^2}{U^2}. \tag{11}$$

In general, U is smaller in the deep ocean than in the upper ocean, so one should be able to use larger γ in the deep ocean. Therefore, γ in general should be a function of depth to achieve “optimal” acceleration.

In summary, the idea of the accelerated convergence method is to reduce the ratio of the diffusive time scale to the wave periods in the distorted system to allow smaller number of time-steps of integration. This interpretation is simply based on the CFL criterion for explicit time differencing and has nothing to do with the frequency bands of the planetary waves. For example, for a given low frequency, both the physical system and the distorted system contain Rossby waves, the only difference is that the wavelengths are different (Bryan, 1984). For the rigid lid system of equations of the GFDL model used in this study, baroclinic gravity and Kelvin waves, not Rossby waves, are the limiting factors in determining the maximum allowable time-step of the explicit integration. So Rossby waves play no role in the new interpretation of the accelerated convergence method.

Customarily in the literature, time for tracers is often defined as $t\gamma$, where t is time for momentum. A time-step Δt for momentum implies a time-step $\Delta t\gamma$ for tracers. Therefore, the implementation of eqs. (3–4) can be accomplished equivalently by integrating the momentum equation and tracer equations asynchronously. The accelerated convergence method is also referred to as asynchronous integration method.

3. Numerical experiments and results

The numerical code used in this study is based on the Bryan–Cox–Semtner model (Semtner, 1974 and Cox, 1984). For unstable stratification, Marotzke’s (1991) complete mixing scheme of convective adjustment, formulated independently by Wang (1993), is used. The model ocean is of box-type with a flat bottom, having the geometry $60^\circ \times 69^\circ \times 5000$ m, with equator being the northern boundary, where symmetric boundary condition is imposed. The symmetric boundary condition implies the actual model domain is twice as large and is subject to symmetric forcing. Therefore the computing costs are reduced by a factor 2. We assumed that the solution is symmetric. The model basin represents the southern half of this symmetric basin. The resolution is $22 \times 25 \times 20$, with uniform zonal and meridional grid sizes of three degrees. This resolution is a little better than Danabasoglu et al.’s (1996) $4^\circ \times 3^\circ$ horizontal resolution and is the typical horizontal resolution of present day climate models. The vertical grid size is 40 m near the surface and gradually increases to 450 m near the bottom. There is no salinity and wind forcing. The thermal forcing is of restoring type with a relaxation time constant of 30 days for the vertical resolution used. The surface restoring temperature is defined by

$$T_* = \frac{T_1(y) + T_2(y)}{2} + \frac{T_1(y) - T_2(y)}{2} \sin\left(\frac{2\pi t}{\text{year}}\right), \tag{12}$$

where

$$\begin{aligned} T_1(y) &= 28 \exp[-(y/45)^2], \\ T_2(y) &= 28 \exp[-(y/60)^2], \end{aligned} \tag{13}$$

y is in degrees latitude; T_1 and T_2 are in degrees Celsius. This seasonal forcing is a very crude approximation of Levitus (1982) climatology. Summer and winter conditions are represented by T_1 and T_2, respectively. Right at the equator, the seasonal forcing amplitude is zero (i.e., no seasonal variation of T_*). At the southern boundary, the amplitude of forcing is about 5°C, which is comparable to the range of the annual variation of surface temperature of Levitus (1982) at 70°S.

Sub-grid scale mixing processes are parameterized using standard constant eddy viscosity and diffusivity coefficients. Horizontal eddy viscosity and diffusivity coefficients are 3×10^9 cm^2/s for momentum and 1×10^7 cm^2/s for heat. Vertical viscosity and diffusivity coefficients are 20 cm^2/s for momentum and 1 cm^2/s for heat, respectively.

To follow the accustomed nomenclature in the literature, we shall refer $\gamma(z)t$ as time for tracers in the numerical experiments. The clock time for forcing follows the "surface time" $\gamma(z_1)$t, where z_1 is the first level for temperature. Experiments with $\gamma \neq 1$ are referred to as asynchronous integration experiments while experiments with $\gamma = 1$ are referred to as synchronous integration experiments.

The numerical experiments, listed in Table 1, consist of one control experiment (control), two asynchronous experiments (A1 and A2), and two synchronous experiments (S1 and S2), which were initialized using the asynchronous equilibrium solutions of A1 and A2, respectively. The initial condition for the control experiment, experiment A1, and A2 is basin-averaged Levitus annual mean climatology for potential temperature and rest for velocity. To facilitate discussion, we adopt the following practical definition of equilibrium: the system is said to reached equilibrium when the annual mean bottom temperature drifts no more than 10^{-8}°C per year (or per surface year for the case of distorted systems). The control experiment is integrated synchronously from rest for 9010 years. Equilibrium is essentially reached after 4700 years of integration, or about 13.7 million time-steps*. Note that the model basin used here is much smaller than that of a global ocean model such that a shorter time is needed to reach equilibrium. In experiment A1, γ increases exponentially from 48 at the surface to 480 at the model bottom, resulting in an equivalent time-step for temperature of 1 day near the surface and 10 days at the bottom. Experiment A1 is integrated for 3000 surface years, or 30 000 bottom years. Equilibrium is reached after 1250 surface years, or about 0.45 million time-steps. The initial condition for experiment S1 is the solution of A1 at surface year 3000. It is integrated for 9010 years synchronously ($\gamma = 1$). Experiment A2 is similar to A1 except that $\gamma = 96$ throughout the water column, or a time-step for temperature of 2 days at all levels. It is integrated for 12 000 years and equilibrium is reached after about 4700 years, or 0.85 million time-steps. The initial condition for experiment S2 is year 12 000 of A2 and it is also integrated synchronously for 9010 years.

Fig. 1 shows January maximum meridional mass transport for the 3 synchronous integration cases (control, S1, and S2), superimposed with the annual cycles of maximum meridional mass transport for the first 50 years of S1 and the last 10 years of all three cases. Because of the enormous range of the time axis, the annual cycles appear in the form of collapsed vertical lines. For exp. S1 (dashed line), January mass transport reached a new steady value after about 3000 years of synchronous integration. The same is true for exp. S2 (dotted line). Control experiment (thick solid line), S1, and S2 all have the same equilibrium. The ranges of annual cycle are identical, as indicated by the three vertical lines that have the same lengths.

* If the equilibrium threshold is reduced to 10^{-7}°C/year or even to 10^{-6}°C/year, the equilibration time would be reduced by 1000–2000 years.

Table 1. *Numerical experiments; time-step for velocity is denoted by Δt_u; time-step for temperature is $\Delta t_T = \gamma \Delta t_u$*

Experiment	Initial condition	Acceleration	Integration length surface/bottom years	Time-step (h)
control	rest	no, $\gamma = 1$	9010	$\Delta t_u = 3.0$
A1	rest	yes, $\gamma = \gamma(z)$	3000/30 000	$\Delta t_u = 0.5$
S1	A1, $t = 3000$ yr.	no, $\gamma = 1$	9010	$\Delta t_u = 3.0$
A2	rest	yes, $\gamma = 96$	12 000	$\Delta t_u = 0.5$
S2	A2, $t = 12\,000$ yr.	no, $\gamma = 1$	9010	$\Delta t_u = 3.0$

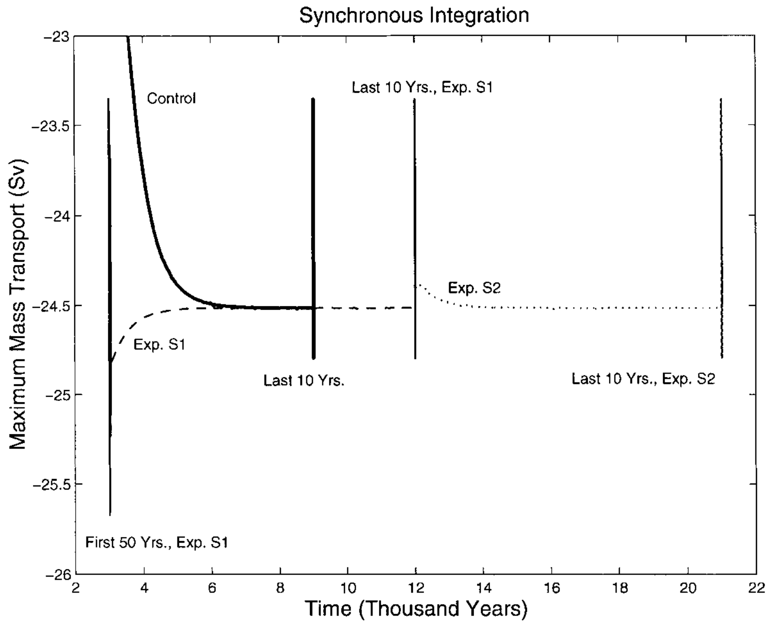

Fig. 1. January maximum meridional mass transport (in Sverdrups, 1 Sv = 10^6 m^3/s) of synchronous integrations. Thick solid line: control; dashed line: Exp. S1; dotted: Exp. S2. Full annual cycles of the first 50 years of S1 and the last 10 years all cases are also shown, which appear in the forms of vertical bars because of the large range of the time axis. Details of the annual cycles are shown in Fig. 2.

Fig. 2 shows maximum meridional mass transport for the first 50 years of synchronous integration experiment S1 (thin solid line), S2 (dashed line), and the last 10 years (years 9000–9010) of S1 (thick solid line). All three cases have the same equilibrium, so only one case is shown. The first 20 years of synchronous integrations show more rapid adjustments than the next 30 years. Near year 50, the adjustments are very slow. But the solutions for S1 and S2 are different from each other and both are different from the true equilibrium solution (thick solid line). This means if different asynchronous integration schemes (or different $\gamma\alpha$s) are used, 50 years of synchronous integration beyond asynchronous equilibria will give different results. The difference in annual mean maximum meridional mass transports is about 0.3 × 10^6 m^3/s. Only after thousands of years of synchronous integration, the two solutions converge to the true equilibrium.

Figs. 3a–c shows temperature at various depths for the first 50 years of experiment S1 (solid line), S2 (dashed line), and the last 10 years (years 9000–9010) of S1 (solid line). The solutions for years 50–9000 are skipped to show clearly the annual cycle and the early stages of synchronous

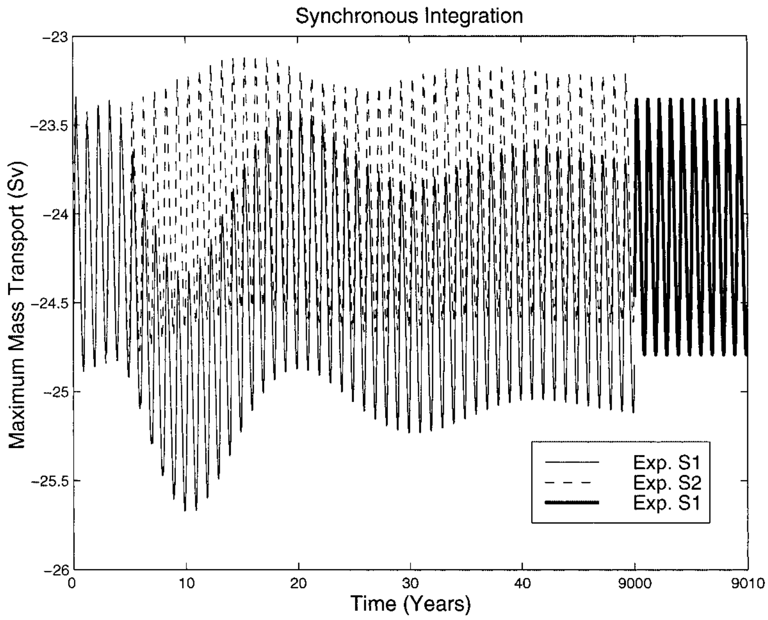

Fig. 2. Maximum meridional mass transports of synchronous integrations. The first 50 years are indicated by the thin solid line (S1) and dashed line (S2). The thick solid line is the equilibrium solution (from years 9000–9010) of S1. Solutions for years 50–9000 are skipped to show the details of the annual cycle. Note that mass transport is for the southern half of the basin, so it is negative.

adjustment. Again, as in meridional mass transport, 2 different asynchronous integration schemes result in different asynchronous equilibria. After 50 years of synchronous integrations beyond the asynchronous equilibrium, the two "near equilibrium" solutions are also different. Only after about 3000 thousand years do S1 and S2 converge to the same equilibrium solution, as shown in Fig. 3d. At shallower depths, the two solutions (S1 and S2) are closer to each other for the first 50 years of synchronous integration (not shown).

Although 50 years of synchronous integration beyond asynchronous equilibria does not yield a new equilibrium, the amplitude of the annual cycle and the annual mean are not very far from the true equilibrium. For example, the difference of bottom temperature (Fig. 3c) between year 50 and year 9000 for S1 is only about 0.01°C. The same is true for S2. The difference of volume averaged temperature between S1 and S2 is about 0.02°C after 50 years of synchronous integrations. In terms of surface heat flux, this seemingly small difference is not very small at all. For example, a uniform surface heat flux of 13 W/m^2 is needed to change the ocean temperature by 0.02°C in a year. Since the adjustment is rather slow, on time scales of thousands of years, for practical purposes there is no need to integrate S1 and S2 to equilibrium. Either the solution of S1 or S2 after 50 years of synchronous integration is good enough.

The key for the accelerated convergence method to work for climate problems with time-dependent forcing is the validity of the hypotheses described in the introduction. Namely, the mean state of the asynchronous equilibrium is close to the mean state of the true equilibrium of the physical system and the mean state of the asynchronous equilibrium is insensitive to the choice of the acceleration parameter. The experiments conducted here provide some anecdotal evidence that supports these hypotheses. However, we cannot prove mathematically one way or the other whether the hypotheses hold or not in general. Analysis of the control experiment at equilibrium can shed some light on this subject. The amplitude of the annual cycle of bottom temperature at high latitude is about 0.01°C. In the ocean interior away from the deep convection region, the amplitude is even smaller.

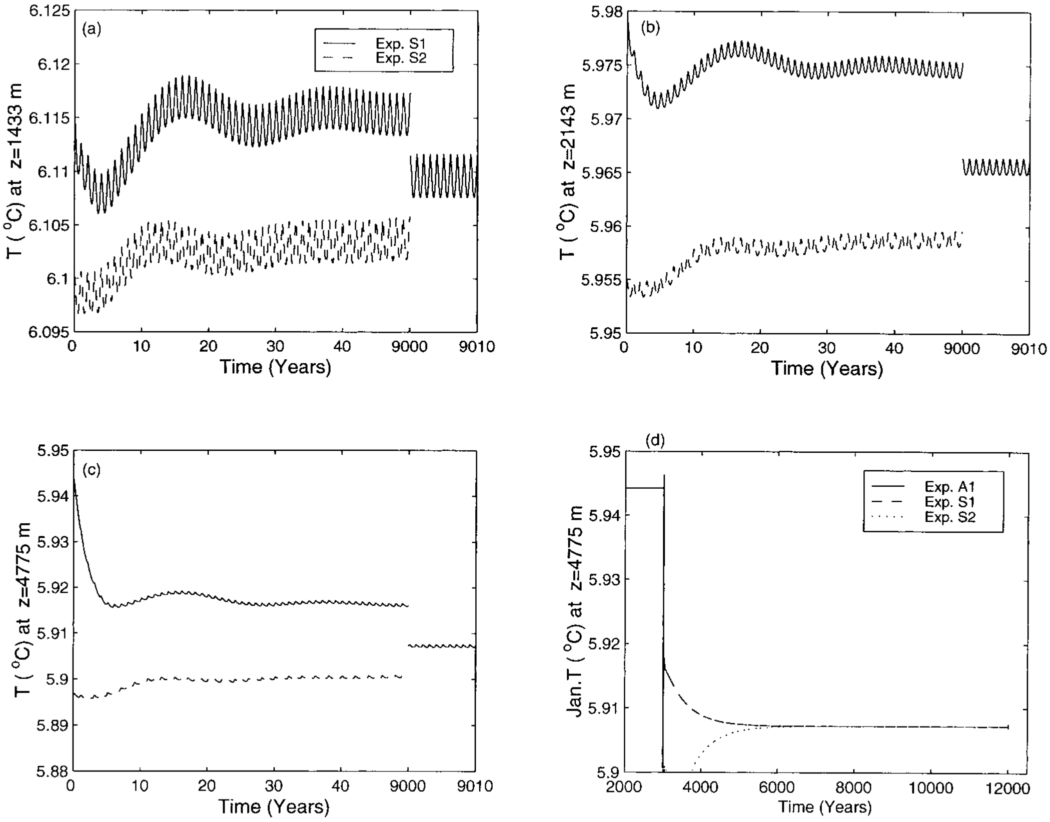

Fig. 3. (a–c): same as Fig. 2, except for temperature at various depths. As in Fig. 2, solutions for years 50–9000 are skipped. (d) January bottom temperature for A1 and S1. The vertical bar at the left is the range of annual variation of asynchronous integration. The small vertical bar at year 12 000 is the range of annual variation of S1 at equilibrium. Note the dramatic difference in the amplitude of the annual cycle between asynchronous and synchronous integrations. Note the the first 3000 years are surface years for A1 and the time axes for S1 and S2 are shifted such that year 3000 means zero for these two cases.

For example, near the equator, the amplitude is 0.0001°C at 1000 m and is only 0.00001°C at bottom. In other words, the solution is practically at a steady state and the equilibrium solution of synchronous integration in the deep ocean behaves like a system subjected to a steady forcing. Under steady forcing, the only assumption needed for the accelerated convergence technique to work is that the system has a unique steady state. Under cyclic forcing, we have shown here that although the equilibrium solutions with different acceleration parameters are different, their annual mean states are very close to each other. The small amplitudes of oscillation in the deep interior ocean is the reason why this is the case. This is also the reason that method of Bryan (1984) works for climate problems with perpetual seasonal forcing.

4. Summary and conclusion

A new simple interpretation of the accelerated convergence method of Bryan (1984) was presented. The acceleration of convergence is achieved by reducing the ratio of the diffusive time scales to the maximum allowable time-step of the distorted system, therefore reducing the number of iterations needed to reach equilibrium.

Idealized thermal spin-up experiments were carried out to address the question whether or not the asynchronous integration method of Bryan (1984) could be applied to climate problems with time dependent forcing. It is found that mean state of the asynchronous equilibrium is a function of the acceleration parameter γ and thousands of years of synchronous integration beyond asynchronous equilibrium is needed to reach new equilibrium. For practical purposes however, these results are more comforting than disturbing because two drastically different asynchronous integrations yielded two mean states of equilibria that are not very far from each other and from that of the true equilibrium, obtained using synchronous integration. As one of the anonymous reviewers pointed out that the differences among runs with different acceleration parameters would be "pale by comparisons to differences that would result from using values for eddy viscosity coefficients and the like". Therefore, 50 years of synchronous integration beyond asynchronous equilibrium seems sufficient for most purposes.

Bryan et al. (1999, manuscript submitted to Journal of Geophysical Research) applied the approach of Danabasoglu et al. in a recent global ocean modeling effort. Synchronous integration of 270 years beyond asynchronous equilibrium in that study still did not yield an equilibrium solution prompted the present study, which is complementary to the study of Danabasoglu et al. (1996). The progress here is that we were able to obtain equilibrium solutions of synchronous integrations. Without obtaining the synchronous equilibrium, whether or not Bryan's (1984) method works for climate models with time-dependent forcing was a lingering question. Although our model configuration is very simplified, it contains the essential elements and correct magnitudes of thermohaline circulation and the qualitative conclusion is likely to hold for global ocean models with realistic seasonal or periodic forcing.

5. Acknowledgments

This study was initiated while the author was a visiting scientist at the National Center for Atmospheric Research, Boulder, Colorado, USA. Conclusion of this study is made possible by the funding of Frontier Research Systems for Global Change through its sponsorship of the International Pacific Research Center (IPRC). Most of the numerical computations were carried out on a Cray-J90se at IPRC. Section 2 was taken from the author's Ph.D. thesis (Wang, 1993), which is funded by the US National Science Foundation under grant OCE-9019580. We thank the two anonymous reviewers for their helpful comments.

REFERENCES

Bryan, K. 1984. Accelerating the convergence to equilibrium of ocean-climate models. *J. Phys. Oceanogr.* **14**, 666–673.

Courant, R., Friedrichs, K. O. and Lewy, H. 1928. Über die partiellen Differenzengleichungen der mathematischen Physik. *Math. Ann.* **100**, 32.

Cox, M. D. 1984. *Geophysical Fluid Dynamics Laboratory Technical Report no. 1*, Princeton.

Danabasoglu, G, McWilliams, J. C. and Large, W. G. 1996. Approach to equilibrium in accelerated global oceanic models. *J. Climate* **9**, 1092–1110.

Levitus, S. 1982. *Climatological atlas of the world's oceans.* NOAA Prof. Paper No. 13, US Govt. Printing Office.

Marotzke, J. 1991. Influence of convective adjustment on the stability of the thermohaline circulation. *J. Phys. Oceanogr.* **21**, 903–907.

Semtner, A. J. 1974. *An oceanic general circulation model with bottom topography.* Tech. Rep. no. 9, Department of Meteorology, University of California, Los Angeles, CA, 99 pp.

Wang, D. 1993. *Modeling deep equatorial circulation.* Ph.D. thesis, University of Hawaii at Manoa, 157 pp.